Astron. Astrophys. 276, 278–288 (1993)

ASTRONOMY AND ASTROPHYSICS

Optical properties of dust aggregates

II. Angular dependence of scattered light

Takashi Kozasa[1], **Jürgen Blum**[2] * **Hajime Okamoto**[3] **and Tadashi Mukai**[3,4]

[1] The Institute of Space and Astronautical Science, Kanagawa 229, Japan
[2] Max–Planck–Institut für Kernphysik, D-69029 Heidelberg 1, Germany
[3] Department of Earth Sciences, Kobe University, Kobe 657, Japan
[4] The Graduate School of Science and Technology, Kobe University, Kobe 657, Japan

Received January 23, accepted April 3, 1993

Abstract. The angular dependence of light scattered by dust aggregates has been investigated by means of the discrete dipole method. Two types of aggregates have been treated; BPCA and BCCA whose fractal dimensions are ~ 3 and ~ 2 in the limit of large size respectively, and whose number of constituent particles range from $N = 256$ to 4096. The radii of constituent particles are 0.01μm and are partly 0.03μm. Two kinds of minerals are considered as the constituents; silicate and magnetite. The calculations have been carried out at the wavelength $\lambda = 0.6\mu$m.

The angular dependence of the degree of linear polarization and the scattered intensity is sensitive to the structure as well as the chemical composition with increasing size of the aggregates. The degree of linear polarization of BCCA shows the behavior similar to that of the individual constituent particles independent of N and of the chemical composition. In BPCA, the maximum value is depressed and the scattering angle at the maximum shifts towards larger scattering angles with increasing N, which is more remarkable in the magnetite aggregates than in the silicate ones. The difference in the behavior of polarization between BPCA and BCCA can be interpreted as the result of multiple scattering in the aggregates reflecting the difference in the structure.

The forward scattering lobe is well-developed with increasing N in BPCA in spite of the smaller size than BCCA with the same number of constituent particles. For a given aggregate, the scattered intensity shows almost the same behavior of angular dependence regardless of, but the strength is sensitive to the chemical composition of the constituent particles. The intensity at the scattering angle $\theta = 0°$ is independent of the structure of the aggregates and is proportional to N^2 in the range of our calculations. The angular dependence of the scattered intensity exhibits a similarity relation when the size parameter of the aggregates $X = kR \gtrsim 3$, where k is the wavenumber and R is the characteristic radius of aggregate. The angular dependence can be divided into at least 4 regimes according to the value of $q = 2kR\sin(\theta/2)$. The scattered intensity in the region of $q \lesssim 2$ is dominated by the coherently scattered light from the constituent particles and well reflects the size and the mass of aggregates, independent of the structure. The distinction between BCCA and BPCA occurs in the region of $2.4 \lesssim q \lesssim 5.0$ through the effect of multiple scattering in the aggregates.

Key words: optical properties – dust aggregates – fractals – interstellar/interplanetary dust

1. Introduction

Dust aggregates are the natural by–products when we consider the evolution of dust particles in space. Observations have suggested presence of dust aggregates in dense molecular clouds as well as pre-solar nebulae (Cardelli et al. 1989; Mathis 1990; Draine 1990), in the interplanetary space (Brownlee et al. 1976; Giese et al. 1978), in cometary atmospheres (Greenberg & Hage 1990), and in planetary and satellite atmospheres (West 1991a). The optical properties of dust aggregates play a key role in considering the chemical and physical processes prevailing at these astrophysical sites, and investigations are also crucial to reveal the nature of dust aggregates in space by comparison with the observations. The measurements of scattering properties, i.e. the angular dependence of the scattered intensity and the degree of linear polarization, in particular have been considered to be a useful method to characterize bodies with fluffy structures, rough surfaces and/or irregularly shapes (Bohren & Huffman 1983). This method is used in many fields of science, industry and technology.

Observationally, the angular dependence of the degree of linear polarization and the scattered intensity of the zodiacal light have revealed the duality of the scattering properties of interplanetary dust particles (IDP) when Mie theory being applied

Send offprint requests to: Jürgen Blum
* Present address: MPG research group "dust in star forming regions" Schillergäßchen 2, D-07745 Jena, Germany

to interpret the data: The degree of linear polarization has a maximum around the scattering angle $\theta = 90°$, which implies that the size of IDP is small in comparison with the observed wavelength. On the other hand, the wavelength dependence of the scattering cross section is neutral and the angular dependence of the scattered intensity shows strong forward scattering, which suggests that IDP are large particles. Compact spherical bodies have failed to reproduce the duality. In fact the dust particles in the stratosphere, part of which are considered to be of interplanetary origin, are assemblages of tiny particles (Brownlee et al. 1976). From this viewpoint, so far many laboratory experiments using natural as well as artificial assemblages of dust particles have been performed in order to characterize the nature of dust in space by comparison with the observations of the zodiacal light and of the scattered light in cometary atmospheres (Giese et al. 1978; Weiss–Wrana 1983; Zerull et al. 1992). Also theoretical calculations have been carried out to reveal the dependence of the scattering properties of dust aggregates on their porosity, surface roughness and structure (Perrin & Sivan 1991; Hage et al. 1991; West 1991b).

The investigation of scattering properties of dust aggregates is very important to deduce the structure, the size and the chemical composition of dust aggregates in space by comparison with observations. Computer simulations using the discrete dipole method (see Draine 1988 for the details) is one of the powerful methods to investigate the optical properties of dust aggregates, because we can examine the optical properties of dust aggregates systematically by changing their structure, size and chemical composition.

Recently we investigated the wavelength dependence of the optical properties of the dust aggregates produced by 3-dimensional Monte–Carlo simulations (Kozasa et al. 1992, hereafter referred to as Paper I). Following Paper I, in this paper we investigate the angular dependence of the scattering properties systematically in order to reveal how the scattering properties of dust aggregates depend on their structure, size and chemical composition. We treat two types of dust aggregates with very different structures, which are composed of 256 to 4096 spherical particles whose radii are 0.01μm. We partly treat the dust aggregates consisting of constituent particles whose radii are 0.03μm. We consider two kinds of minerals as the constituent particles: silicate as an example of dielectric materials and magnetite as an absorbing material. Also we investigate the effect of the mixing of silicate and magnetite constituent particles for both types of aggregates with $N = 2048$.

We describe the method of the calculations and the dust aggregates used in the calculations in Sect. 2. The angular dependence of the degree of linear polarization is presented and discussed in Sect. 3. The results of calculations of the angular dependence of the scattered intensity are summarized first in Sect. 4. Then we investigate the dependence of the behavior on the size and the structure of dust aggregates, comparing the results by the discrete dipole method with the results of calculations based on two simple models neglecting the effect of multiple scattering; (A) a homogeneous sphere model and (B) a fractal model with an assumed two point correlation function. The concluding remarks are presented in Sect. 5.

2. The dust aggregates and the method of calculation

The dust aggregates used in this paper were produced by the same method described in Paper I. We had to extend the number of constituent particles up to 4096 in order to investigate clearly the dependence of the scattering properties on their size and structure. The Ballistic Cluster–Cluster Aggregates (BCCA), whose fractal dimension is ~ 2 in the limit of large size, were continuously grown up to $N = 4096$ by adding clusters to BCCA with $N = 1024$ used in Paper I, while the Ballistic Particle–Cluster Aggregates (BPCA), for which $D \sim 3$ in the limit of large size, were newly produced.

Table 1. The quantities that characterize the dust aggregates used in the calculations. Note that the radius of constituent particle $a_0 = 0.01\mu$m. The characteristic radius $a_c = \sqrt{5/3}R_g$ where R_g is the radius of gyration of the aggregate, a_s the geometric cross section equivalent radius, a_m the mass equivalent radius, and P the porosity. The fractal dimensions $D \sim 3$ for BPCA and ~ 2 for BCCA in the limit of large size, which are determined by the method of radius of gyration. The values D_f and ξ are the fractal dimension and the cut-off parameter derived by fitting the scattered intensity by the fractal model (see the text)

Ballistic	Particle–Cluster		Aggregates	(BPCA)		
N	a_c (μm)	a_s (μm)	a_m (μm)	P	D_f	ξ
256	0.1280	0.1096	0.0635	0.8779	2.98	0.37
512	0.1609	0.1423	0.0800	0.8771	3.00	0.38
1024	0.2037	0.1880	0.1008	0.8788	3.00	0.38
2048	0.2537	0.2455	0.1270	0.8745	3.00	0.38
4096	0.3194	0.3160	0.1600	0.8743	3.00	0.37
Ballistic	Cluster–Cluster		Aggregates	(BCCA)		
N	a_c (μm)	a_s (μm)	a_m (μm)	P	D_f	ξ
256	0.2049	0.1241	0.0635	0.9703	2.99	0.42
512	0.4244	0.1741	0.0800	0.9933	2.24	0.46
1024	0.5320	0.2340	0.1008	0.9932	2.17	0.55
2048	0.6729	0.3311	0.1270	0.9933	2.25	0.52
4096	0.9929	0.4499	0.1600	0.9958	2.25	0.48

Table 1 summarizes the quantities that characterize the dust aggregates used in the present calculations, where the radii of constituent particles are 0.01μm. The characteristic radius a_c of an aggregate is defined by $a_c = \sqrt{5/3}R_g$ where R_g is the radius of gyration. Both aggregates consisting of $N = 4096$ spherical particles projected on a plane are presented in Figs. 1a and 1b; both figures are in the same scale. BPCA have more compact and homogeneous structure in comparison with BCCA which show the very porous and fluffy structure.

The angular dependence of the scattered light is calculated by means of discrete dipole approximation (DDA) by modifying

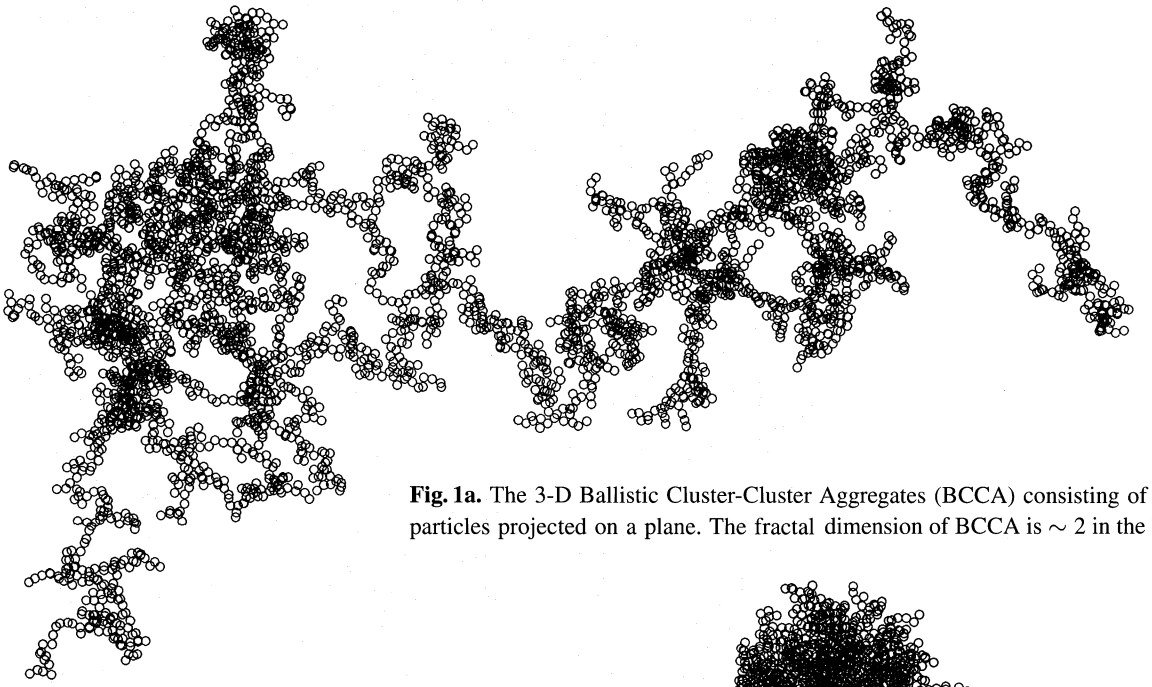

Fig. 1a. The 3-D Ballistic Cluster-Cluster Aggregates (BCCA) consisting of $N = 4096$ spherical particles projected on a plane. The fractal dimension of BCCA is ~ 2 in the limit of large size

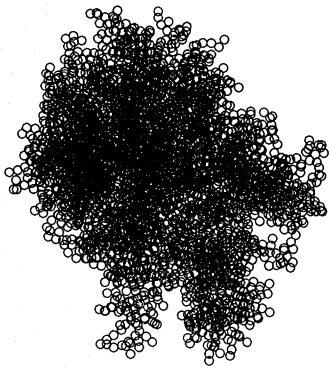

Fig. 1b. The same as Fig. 1a, but for BPCA whose fractal dimension is ~ 3 in the limit of large size. Figures 1a and 1b are in the same scale. BPCA is much smaller in size and more compact in structure than BCCA

the original program coded by Draine and Flatau (see Goodman et al. 1991) so that we can treat a dust aggregate whose constituent particles are not located on a cubic lattice. Usually the discrete dipole method have been applied by dividing a compact body into subvolumes (dipoles). For dust aggregates, however, we regard a constituent particle as a subvolume (a dipole) to avoid the artificial enhancement of the cross sections of light interaction caused by dividing the constituent particle into insufficient number of subvolumes. In this method, the size a_i of the i–th constituent particle with the complex refractive index m_i is limited so as to be $|m_i|ka_i \lesssim 0.6$, in order to keep the relative deviation within 10%, where the wavenumber $k = 2\pi/\lambda$ and the wavelength is λ (see Paper I for the details). In our calculations, the effective polarizability α_i of i–th constituent particle is defined by

$$\frac{1}{\alpha_i} = \frac{1}{\alpha_i^0} - \frac{2}{a_i^3}[(1 - ika_i)\exp(ika_i) - 1] \tag{1}$$

and

$$\frac{1}{\alpha_i} = \frac{1}{\alpha_i^0} - \left(\frac{k^2}{a_i} + \frac{2}{3}ik^3\right) \quad \text{for } ka_i \ll 1 \tag{2}$$

where $\alpha_i^0 = [(m_i^2 - 1)/(m_i^2 + 2)]a_i^3$.

This expression of the effective polarizability automatically includes the *radiative reaction* term introduced by Draine (1988) and the additional *non-radiative* term, the first term in the bracket of Eq. (2). Both terms arises from the interaction of a constituent particle with itself under the assumption that the electric field inside the constituent particle is uniform (Hage & Greenberg 1990). Recently Draine & Goodman (1992) investigated the effect of the inclusion of additional *non-radiative* term extensively, and they concluded that the inclusion of this term improves the accuracy of the discrete dipole method when $|m^2 - 1| > 5$ for a sphere with the complex refractive index m.

For a dust aggregate consisting of N constituent particles whose positions and induced dipole moments are specified by $\boldsymbol{r}_j$ and $\boldsymbol{P}_j$ ($j = 1$ to N), the scattered intensities $i_1(\theta)$ and $i_2(\theta)$, perpendicular and parallel to the scattering plane respectively, are calculated by

$$i_{1,2}(\theta) = \frac{k^6}{2\pi|\boldsymbol{E}_0|^2}\int_0^{2\pi} d\varphi \left|\sum_{j=1}^{N}[\boldsymbol{P}_j - \boldsymbol{n}(\boldsymbol{n}\cdot\boldsymbol{P}_j)]_{1,2} \times \exp(-ik\boldsymbol{n}\cdot\boldsymbol{r}_j)\right|^2, \tag{3}$$

where $|\boldsymbol{E}_0|$ is the amplitude of incident light, $\boldsymbol{n}$ is the unit vector parallel to the direction of scattering, θ is the scattering angle, and φ is the azimuthal angle. Then the scattered intensity $i(\theta)$ and the degree of linear polarization $P(\theta)$ are given by

$$i(\theta) = \frac{i_1(\theta) + i_2(\theta)}{2}, \tag{4}$$

and

$$P(\theta) = \frac{i_1(\theta) - i_2(\theta)}{i_1(\theta) + i_2(\theta)}. \tag{5}$$

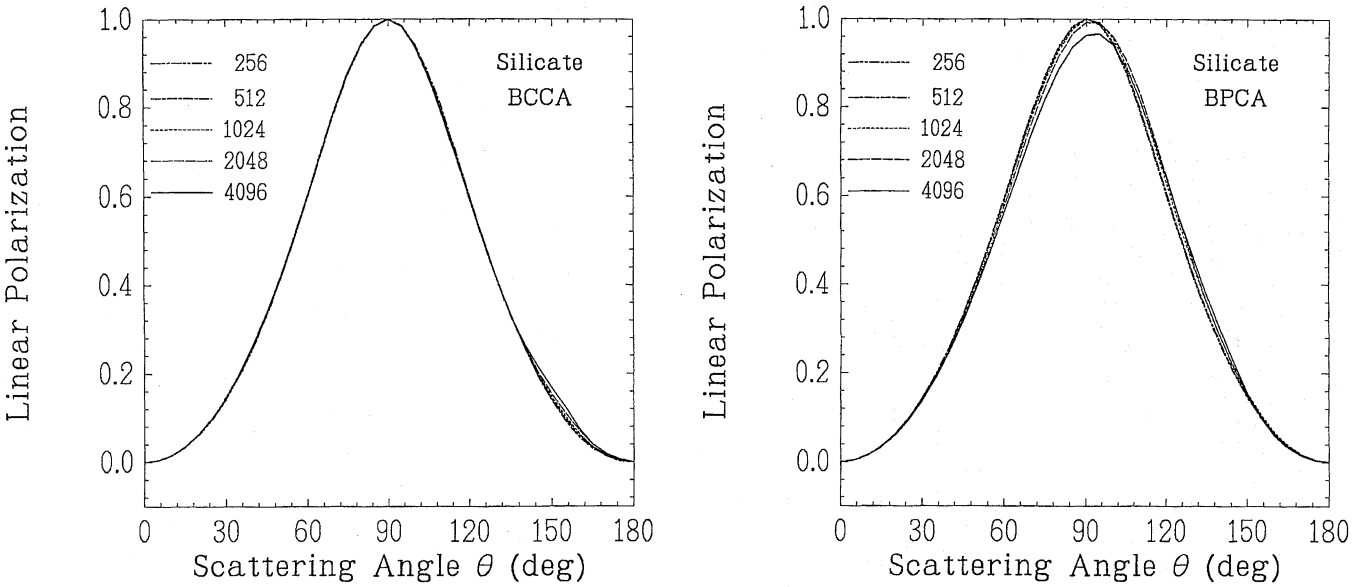

Fig. 2a and b. a (left); the degree of linear polarization of BCCA consisting of N = 256 to 4096 silicate particles at wavelength λ = 0.6μm; The radii of the constituent particles are 0.01μm. **b** (right); the same as **a**, but for silicate BPCA

The scattered intensity as well as the degree of linear polarization in the backward directions are strongly dependent on the direction of incident light and on the configuration of dust aggregates with increasing size of aggregates, as pointed out by Hage (1990). Thus we calculated these values by averaging over the 21 different configurations by rotating the aggregates around three orthogonal directions of the propagation of incident light and by averaging over the azimuthal directions. The interval of the scattering angle is 5° in the present calculations.

The calculations have been carried out at the wavelength λ = 0.6μm for the aggregates in which the radius of the constituent particles a_0 = 0.01μm. Also, partly we have treated BPCA consisting of silicate constituent particles whose radii are 0.03μm in order to reveal the dependence of the scattered intensity on their structure and size of dust aggregates by making the sizes of BPCA large and comparable to those of BCCA. The optical constants of silicate and magnetite are taken from the table of Mukai (1990). As it can be seen from Table 1, the size parameter $x = ka_0$ of the constituent particles is 0.105, and the size parameters $X = ka_c$ of the aggregates range from 1.34 to 3.34 for BPCA, and 2.15 to 10.4 for BCCA when the radii of the constituent particles are 0.01μm.

3. The degree of linear polarization

The angular dependence of the degree of linear polarization of a compact spherical particle is a diagnostic of the size and the chemical composition; the angular dependence has the characteristic features according to the size and to the complex refractive index. However this is not always true for dust aggregates. Figures 2a and 2b show the angular dependence of the degree of linear polarization for BCCA and BPCA consisting of N = 256 to 4096 silicate constituent particles whose radii are 0.01μm, respectively.

The aggregates with N = 256 show the same angular dependence of linear polarization as that of the constituent particle, independent of the structure. In spite of increasing size of the aggregates, BCCA keep the maximum at θ = 90°, and the angular dependence is the same as that of the constituent particle independent of N, except for the backward directions in the large sized aggregates. The deviation from the constituent particle in the backward directions becomes more significant as the number of constituent particles increases. This is also true for magnetite BCCA although the maximum of the degree of linear polarization deviates very slightly from that of the constituent particle. It should be noted that this result does not imply the scattering properties of this type of aggregates are simply interpreted as the sum of the independent scatterers (see Sect. 4). With increasing size parameter in BPCA, the scattering angle at the maximum polarization shifts towards larger scattering angles. The shift of scattering angle at the maximum accompanies the increase and the decrease of the degree of linear polarization in the backward and the forward directions, respectively, in comparison with that of the constituent particle. Also the maximum value becomes depressed with increasing size. These behaviors are more remarkable in magnetite BPCA than in silicate BPCA, as shown in Fig. 2c. Here it should be noted that the variation of the maximum polarization for the mean values of the direction of incident light is less than 1% for the silicate aggregates and is less than 3% at the worst for the magnetite aggregates.

These results of calculations show that the behavior of the linear polarization of dust aggregates cannot be a diagnostic of the size and chemical composition when aggregates have very porous and fluffy structure such as BCCA and also when the size parameter of dust aggregates $X = ka_c \lesssim 1$ regardless of

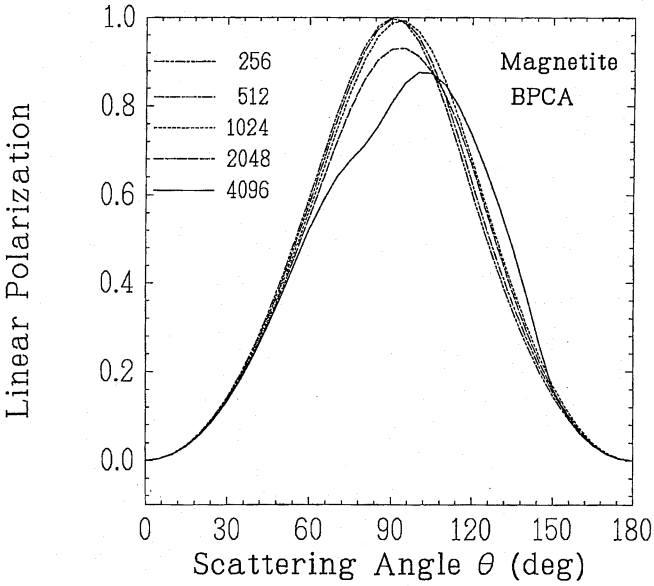

Fig. 2c. The same as Fig. 2-a, but for magnetite BPCA

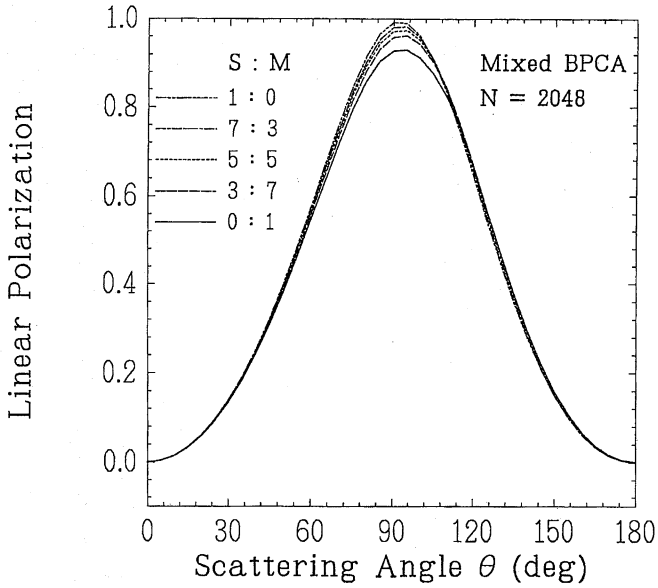

Fig. 3. The degree of linear polarization of BPCA with N = 2048 for which silicate and magnetite constituent particles are randomly mixed with the given ratios. The radii of constituent particles are 0.01μm. The labels "S" and "M" denote silicate and magnetite, respectively

the structure. On the other hand, in BPCA with denser and more homogeneous structure, the behavior reflects the difference in the size and the chemical composition of dust aggregates as the number of constituent particles increases, but the dependence is not so clear, different from the case of a compact spherical body.

The dependence of the behavior of the linear polarization of BPCA on the chemical composition of constituent particles can be clearly demonstrated by mixing silicate and magnetite constituent particles randomly and by changing the ratio in number (hereafter this type of aggregates is referred to as mixed aggregates). Figure 3 shows the result of the calculations for mixed BPCA with N = 2048. As the number ratio of magnetite to silicate constituent particles increases, the maximum of linear polarization systematically decreases, the maximum position being kept around $\theta = 90°$. Thus the depression of the maximum of linear polarization for a given aggregate structure is closely related with the chemical composition of the constituent particles. Here it should be noted that the shape of scattered intensity perpendicular to the scattering plane is almost independent of the chemical composition of aggregates with a given size and structure (see Fig. 5b). However, the shape around the dip and the dip position in the parallel component vary according to the size and chemical composition. This behavior of the scattered intensities causes the difference in the behavior of the degree of linear polarization of BPCA reflecting their size and chemical composition, in the range of the present calculations.

BPCA have denser and more homogeneous structure than BCCA, and magnetite is more absorbing than silicate. Thus, the result of calculations seems to suggest a relation of the behavior of the linear polarization with the optical thickness of the dust aggregates reflecting their structure and chemical composition. However this is not true: The optical thickness defined in Paper I is very small ($\sim 2\times10^{-5}$) for the silicate BPCA with N = 4096, and the aggregate exhibits a noticeable deviation of the behavior of linear polarization from that of the constituent particle. The maximum of the linear polarization is depressed remarkably from 1.

Generally, the behavior of the degree of linear polarization can be explained in terms of the internal and surface scattering processes including diffraction, reflection and refraction, and of the resulting interference of the scattered light. Therefore, the maximum of the degree of linear polarization is expected to be more depressed with increasing size of bodies composed of transparent materials such as silicate because the incident light can penetrate into and the scattered light can escape from the scattering bodies without significant absorption. For absorbing bodies such as magnetite the depression of the maximum tends to be saturated with increasing size of the bodies where the incident and scattered light are absorbed efficiently. The laboratory experiments (Giese et al. 1978; Weiss–Wrana 1983) have confirmed this general trend for bodies with fluffy structure, which seems to be contradictory to the result of present calculations. However we cannot compare the result of the calculations directly with the experimental results because the size of dust aggregates treated here is still smaller than those used in the experiments. Also, partly being consistent with the result of the present calculations, a recent laboratory experiment for a dust aggregate by Zerull et al. (1992) has shown that the maximum of the degree of linear polarization decreases first and then turns to increase as the dust aggregate is coated by an opaque material.

The important result of our calculation is that the behavior of the linear polarization not only depends on the chemical composition but also strongly depends on the size and the structure of the dust aggregates. The behavior of the degree of linear polarization of dust aggregates could be interpreted as the resulting

interference of internally scattered light. The effect of multiple scattering in aggregates could be more dominant in BPCA with dense structure than in BCCA with porous and fluffy structure. As discussed by Berry & Percival (1986) under the assumption of a mean field approximation, the effect of multiple scattering is negligibly small for aggregates whose size parameter $X \ll 1$. For aggregates with $X \gg 1$, the difference in the size, structure and chemical composition being taken into account, the effect of multiple scattering is roughly estimated by the value

$$\eta \sim \left(\frac{a_0}{a_c}\right)^2 N 4ka_0 \left|\frac{m^2-1}{m^2+2}\right| \propto N^{1-2/D} 4ka_0 \left|\frac{m^2-1}{m^2+2}\right| \quad (6)$$

The right hand side of Eq. (6) is valid for dust aggregates whose fractal dimension $D > 2$. The value η increases with increasing N for dust aggregates with fractal dimension $D > 2$, and is independent of N for aggregates of $D \leq 2$ because the incident light on the aggregates in principle illuminates all the constituent particles. Although the size parameters $X = ka_c$ of the dust aggregates used in the present calculation do not always satisfy the condition $X \gg 1$, the value $\eta < 0.05$ for silicate and magnetite BCCA, while $\eta > 0.05$ and increases with increasing N in BPCA. Thus the difference in the behavior of linear polarization between BPCA and BCCA seems to be related with the effect of multiple scattering in the aggregates. However the value η cannot be quantitatively related with the difference in the degree of depression of the maximum polarization between silicate and magnetite BPCA; the value η increases from ~ 0.05 to 0.12 for silicate BPCA and 0.11 to 0.29 for magnetite BPCA as the number of constituent particles increases from $N = 256$ to 4096.

The interpretation of the behavior of linear polarization is not so simple. It should be kept in mind that the size of the constituent particles is also an important parameter to control the behavior of the degree of linear polarization as demonstrated by West (1991b). A laboratory experiment has shown that for aggregates consisting of constituent particles up to 4 the degree of linear polarization decreases with increasing number of constituent particles, but the characteristic features of the constituent particle are kept remaining (see Bohren & Huffman 1983). More extensive laboratory experiments as well as theoretical investigations are needed in order to relate the behavior of linear polarization quantitatively with the size, structure and chemical composition of dust aggregates.

4. The scattered intensity

4.1. The dependence on the structure, size and chemical composition

Figures 4a and 4b (the solid curves) show the angular dependence of the scattered intensity of silicate BCCA and BPCA, respectively. First it should be noted that, different from the angular dependence of the degree of linear polarization, the angular dependence of scattered intensity is not symmetric for BCCA and small sized BPCA. Even for very porous and fluffy aggregates such as BCCA, the scattering properties of the aggregates cannot be interpreted as the sum of the coherent scattering from the individual constituent particles when the size parameter of dust aggregates $X \gtrsim 1$ as shown in Paper I. It should be kept in mind here that the angular dependence of both linear polarization and scattered intensity of dust aggregates all over the scattering angle region $\theta = 0°$ to 180° cannot be reproduced at the same time by any homogeneous spheres with radii equivalent to characteristic radii of dust aggregates, except for dust aggregates whose size parameters are $X \ll 1$.

The angular dependence of the scattered intensity of BPCA with denser and almost homogeneous structure is characterized by the well-developed forward scattering lobe. Then with increasing scattering angle, the intensity decreases gradually and becomes constant in the backward directions as the number of constituent particles increases. On the other hand, in BCCA, the scattered intensity gradually decreases with somehow oscillations as the scattering angle increases, and then the scattering tends to be isotropic. The region of the isotropic scattering is more remarkable in BCCA than BPCA, corresponding to the larger size of BCCA. The intensity in the isotropic scattering region is roughly proportional to N for BCCA, but not for BPCA. The scattered intensity in the backward directions is more depressed in BPCA than in BCCA with the same number of constituent particles. The enhancement of backward scattering of BCCA is more significant with increasing size of the aggregates than BPCA. However the degree of enhancement of the backward scattering is not always an indicator of the size of dust aggregates.

Generally the scattered intensity in the backward directions somehow fluctuates depending on the direction of incident light as well as on the configuration of dust aggregates; the variation of the scattered intensity for a given direction of incident light from the mean values increases as the size of aggregates and the scattering angle increase. In the region of $X \sin(\theta/2) \leq 1$, i.e. in the diffraction lobe defined in Sect. 4.2, the variation is less than 1% of the mean values. For the largest aggregate BCCA with $N = 4096$, the variations reach 8% at $\theta = 90°$ and up to 40% at $\theta > 160°$. Although the overall structure of the angular dependence of the scattered intensity is almost independent of the direction of incident light, the behavior and degree of the enhancement of backward scattering is different from an aggregate to another even if the sizes of aggregates are comparable.

The relative intensity $i(\theta)/i(0)$ of the scattered light is not sensitive to the change of the chemical composition of the constituent particles. This is also demonstrated by mixing silicate and magnetite constituent particles in the same manner as the case of the polarization. Figures 5a and 5b show the scattered intensities perpendicular $i_1(\theta)$ and parallel $i_2(\theta)$ to the scattering plane for mixed BCCA and BPCA with $N = 2048$. The intensities of the scattered light increases as the number of magnetite constituent particles increases. The perpendicular component has the similar angular dependence independent of the number ratio of silicate to magnetite constituent particles (i.e. the chemical composition) for a given type of aggregate, except for

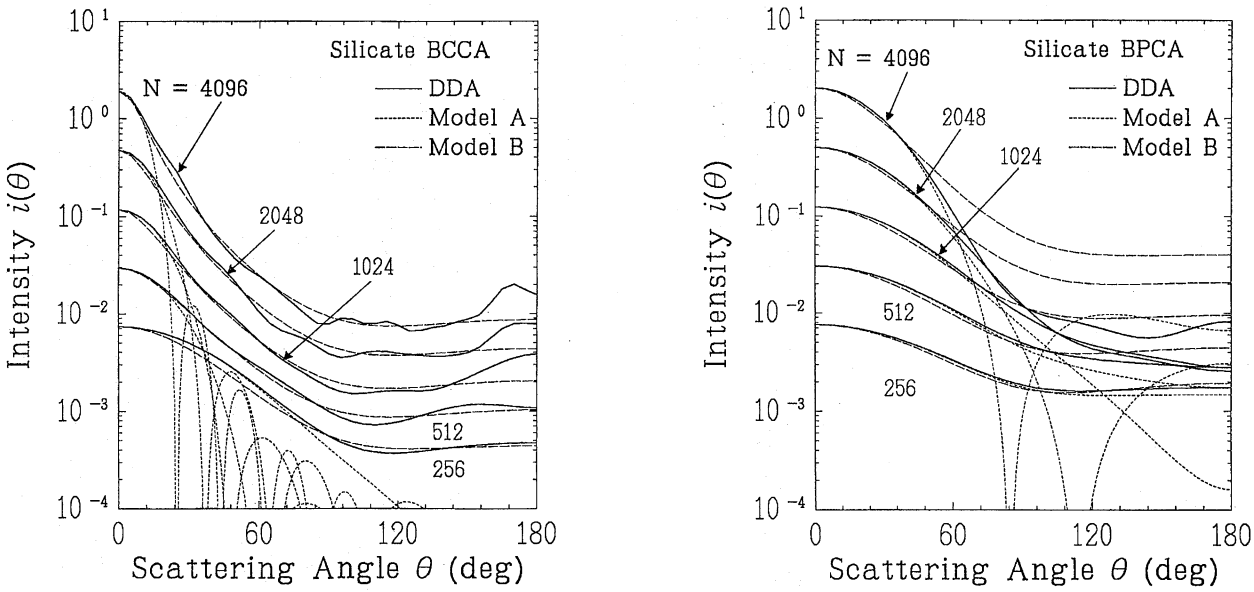

Fig. 4a and b. a (left); the angular dependence of the scattered intensity for silicate BCCA in which the radii of constituent particles are 0.01μm. The result of DDA calculations are represented by the solid curves. The dotted and dashed curves represent the scattered intensities calculated by the homogeneous sphere model (model A) and the fractal model (model B), respectively (see the text). In both models, we assume that the multiple scattering is negligible. **b** (right); the same as **a**, but for silicate BPCA

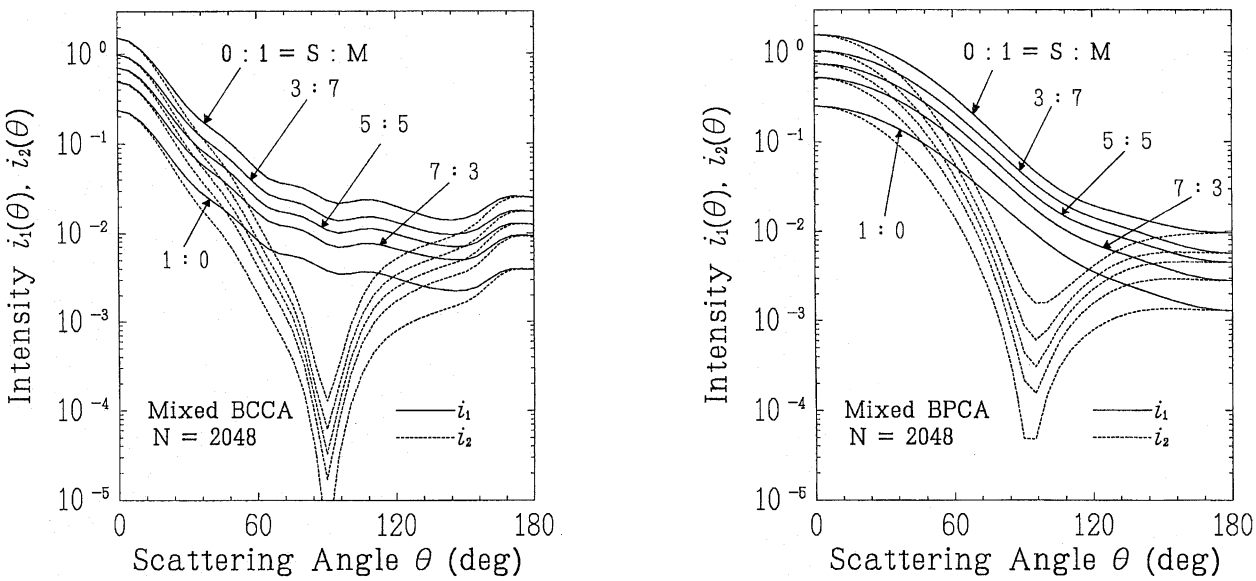

Fig. 5a and b. a (left); the angular dependence of the scattered intensities perpendicular $i_1(\theta)$ and parallel $i_2(\theta)$ to the scattering plane for mixed BCCA with $N = 2048$ for which silicate and magnetite constituent particles are randomly mixed with the given ratios. The radii of constituent particles are 0.01μm. The labels "S" and "M" denote silicate and magnetite respectively. **b** (right); The same as **a**, but for mixed BPCA with $N = 2048$

the backward directions in BPCA. The parallel component of BCCA has the angular dependence similar to that of the constituent particle with the dip at $\theta = 90°$, irrespective of the chemical composition. The intensity at the dip increases with increasing number of magnetite constituent particles. On the other hand, in BPCA the shape around and the position as well as the intensity at the dip of the parallel component vary according to the chemical composition. The total scattered intensity around the dip is dominated by the perpendicular component, which is true for all dust aggregates treated in the present calculations. As the result the behavior of the relative intensity is almost independent of the chemical composition for an aggregate with a given structure and size.

As it can be seen from Figs. 4a and 4b (the solid curves), the intensity at the scattering angle $\theta = 0°$ is almost proportional to N^2 regardless of the structure. Figure 6 shows the dependence of

the intensity at $\theta = 0°$ on the number of the constituent particles for both types of aggregates consisting of silicate and magnetite constituent particles. For smaller sized aggregates, the intensity is slightly larger in BPCA than BCCA. The intensity of BCCA increases in proportion to N^2 with increasing N. However, the intensity of BPCA deviates a little from the N^2 – dependence with increasing N; the intensity is enhanced in silicate BPCA and is depressed in magnetite BPCA, reflecting the difference of the chemical composition. The scattered intensity at $\theta = 0°$ well reflects the mass of the dust aggregates with a given chemical composition through the N^2 – dependence in the range of present calculations.

The results of the calculations demonstrate that the angular dependence of the scattered intensity more definitively reflects the difference in the structure of the aggregates than the behavior of the linear polarization as the number of constituent particles increases, almost independent of the chemical composition. Furthermore, the relative intensity $i(\theta)/i(0)$ shows a similarity as a function of both the size of aggregate and the scattering angle, reflecting the structure of the aggregates, when the size parameter $X \gg 1$. This similarity relation can be shown clearly by plotting the value $i(\theta)q^3/i(0)$ against $q = 2kR\sin(\theta/2)$, where $R = a_c$ and in what follows we represent the characteristic radius of aggregate a_c by R for convenience. Figure 7 shows the relation for silicate BPCA and BCCA respectively. Note that in the figure the radii of the constituent particles in BPCA are 0.03 μm in order to make the characteristic sizes of BPCA large and comparable to the sizes of BCCA. The behavior of $i(\theta)q^3/i(0)$ is almost similar for a given type of aggregates independent of the size of aggregates, except for the smallest BCCA with $N = 256$. Also the behavior clearly distinguish BCCA and BPCA, well reflecting the difference in the structure of the aggregates. Thus this type of plot is useful to characterize the nature of dust aggregates by measuring the angular dependence of scattered intensity.

From Fig. 7 we can divide the angular dependence of the scattered intensity into several regimes according to the value of the nondimensional quantity $q = 2kR\sin(\theta/2)$ when the size parameter of aggregates $X = kR \gtrsim 3$: In the region of $q \lesssim 1$, the relative intensity of the scattered light is independent of the structure as well as the size of the aggregates as a function of q. Following the transition region of $1 \lesssim q \lesssim 2$, the scattered intensity generally decreases in proportion to $q^{-\gamma}$. In the region of $2.4 \lesssim q \lesssim 5.0$, the relative intensity shows the distinctive behavior reflecting the difference in the structure between BCCA and BPCA, except for BCCA with $N = 256$; $\gamma - 3 < 0$ for BCCA and $\gamma - 3 > 0$ for BPCA. Although the value γ fluctuates from an aggregates to another, the value γ is in the range of ~ 1.5 to 2 for BCCA and of ~ 5 to 6 for BPCA. Afterwards the scattered intensity decreases in proportion to q^{-3} with oscillating in the region of $5 \lesssim q \lesssim q_c$, irrespective of the structure of dust aggregates. The dividing value q_c increases with increasing size of dust aggregates, but the oscillation of the scattered intensity prevents us from determining the value exactly. In the region of $q_c \lesssim q \leq 2kR$, the scattering tends to be isotropic with oscillations and a significant enhancement of the backward scattering.

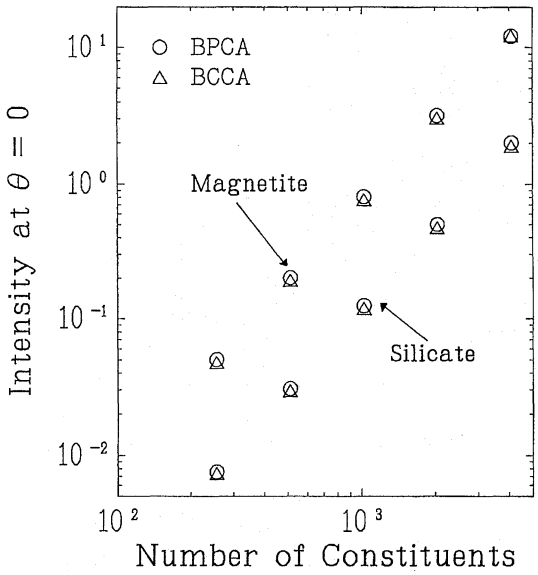

Fig. 6. The scattered intensity $i(\theta)$ at $\theta = 0°$ versus the number of the constituent particles for BPCA and BCCA. The radii of constituent particles are 0.01μm

4.2. Comparison with simple models

The angular dependence of the scattered light is a more definitive indicator of the structure and the size of dust aggregates irrespective of the chemical composition as shown in the previous sections. In order to clarify how the angular dependence of the scattered light reflects the difference in the size and the structure of dust aggregates, in this section, we investigate the behavior of angular dependence of the scattered intensity, comparing the results by the discrete dipole method with those by simple models.

We consider two models: (A) The constituent particles are homogeneously distributed throughout a sphere of radius $R = a_c$. (B) The constituent particles are isotropically distributed in a sphere of radius R with a given two point correlation function in order to take into account the structure of aggregates. For simplicity, we assume in both models that the effect of multiple scattering is negligible.

In model A, the phase difference being taken into account by analogy to the Rayleigh–Gans scattering, the scattered intensity under the assumption of a mean field approximation is given by

$$i(\theta) = N^2 k^6 |\alpha|^2 \frac{(1+\cos^2\theta)}{2} \left[\frac{3(\sin q - q\cos q)}{q^3}\right]^2, \quad (7)$$

where α is the effective polarizability of the constituent particles defined by Eq. (1), and $q = 2kR\sin(\theta/2)$. For model B, according to Berry & Percival (1986) and Teixeria (1986), we assume the two point correlation function, i.e. the probability

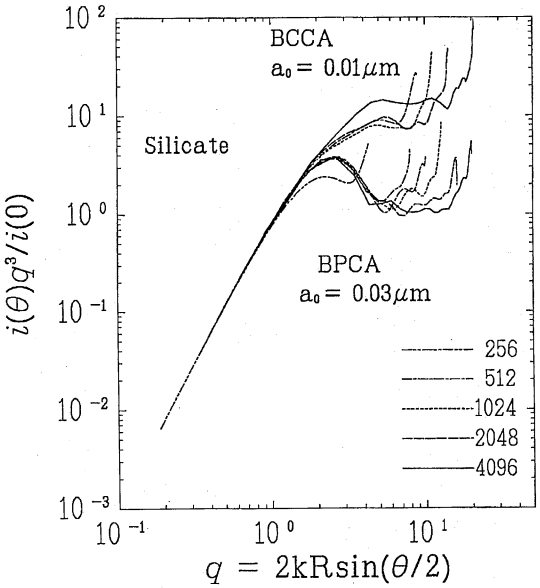

Fig. 7. The value $i(\theta)q^3/i(0)$ versus $q = 2kR\sin(\theta/2)$. Note that the radii of constituent particles of BPCA are 0.03μm

that other constituent particles can be found within the radius of r from a given constituent particle, is given by

$$f(r/R) = \frac{N}{4\pi R^3}\frac{1}{\Gamma(D_{\rm f})\xi^{D_{\rm f}}}\left(\frac{r}{R}\right)^{D_{\rm f}-3}\exp(-r/\xi R), \qquad (8)$$

where $D_{\rm f}$ is the fractal dimension, ξ is a cutoff parameter, and Γ is the gamma–function. Then the scattered intensity is given by

$$i(\theta) = Nk^6|\alpha|^2\frac{(1+\cos^2\theta)}{2}\Big[N+ (N-1)\frac{\sin[(D_{\rm f}-1)\tan^{-1}(\xi q)]}{(\xi q)^{D_{\rm f}}(D_{\rm f}-1)[1+(1/\xi q)^2]^{(D_{\rm f}-1)/2}}\Big]. \qquad (9)$$

According to the difference in the structure of aggregates, in this model the radial distribution of constituent particles in the aggregates is represented by the two parameters; the fractal dimension $D_{\rm f}$ and the cutoff parameter ξ, which are determined by fitting the angular dependence of the scattered intensity with that by DDA calculations.

Both models give the same intensity at $\theta = 0°$ and the intensity is proportional to N^2 as shown in Sect. 4.1. However the intensity at $\theta = 0°$ given by the models is smaller than the result of the DDA calculations, which might be due to the less screening effect of the aggregates. In the following, we adjust the intensity at $\theta = 0°$ to that of DDA calculations. The scattered intensity calculated by both models are shown in Figs. 4a and 4b together with the results of DDA calculations; the dotted curves by the homogeneous model A and the dashed curves by the fractal model B.

The homogeneous model A specified by Eq. (7) well reproduces the calculated scattered intensity in the region of $q \lesssim 2$ irrespective of the structure of aggregates; more strictly up to the point of inflection in the forward scattering lobe. The homogeneous model A is a good approximation for the angular dependence of the scattered intensity of the small sized aggregates whose size parameter $X \lesssim 1$, regardless of the structure. In the region of $q > 2$, the model A develops the patterns due to the interference of scattered light with increasing size of scattering bodies, and cannot reproduce the results of the DDA calculations. In BCCA the well-fitted region is confined to the region of very small scattering angle owing to the larger size in comparison with BPCA. The comparison of the results of DDA calculations with those of the model A implies that the scattered intensity in the region of $q \lesssim 2$ is dominated by the coherent scattering light from the individual constituent particles in the aggregates. Thus the shape and intensity of the scattered light in this region well reflect the size as well as the mass of the dust aggregates irrespective of the structure. Therefore we can regard the well-fitted region in the large sized aggregates as "the diffraction lobe" in analogy with the geometric optics. As the value of q increases, the incoherent scattering dominates the scattering process in the dust aggregates. In comparison with a compact sphere, the scattered light less destructively interferes each other reflecting the non-homogeneous structure of the aggregates, and then the homogeneous model A fails to reproduce the result of DDA calculations.

The angular dependence of the scattered intensity calculated by the model A is almost the same as that calculated by using the Maxwell–Garnett mixing rule and Mie theory. Thus the application of the Maxwell–Garnett mixing rule with Mie theory is an efficient method to calculate the scattering cross sections of and the radiation pressure forces acting on the dust aggregates such as BPCA which have the well-developed "diffraction lobe", as shown in Paper I and Mukai et al. (1992).

The radial distribution of constituent particles in the aggregates being taken into account, the model B well reproduces the calculated scattered intensity of BCCA all over the scattering angles of $\theta = 0°$ to $180°$, with the fitting parameters $D_{\rm f}$ and ξ tabulated in Table 1. The derived fractal dimensions $D_{\rm f}$ vary from an aggregate to another, and are also significantly different from the fractal dimension D derived from the method of radius of gyration in the limit of large size. Particularly for the smallest BCCA, the derived fractal dimension $D_{\rm f}$ is very different from other aggregates. However, this may be inevitable, partly because the determination of fractal dimension D using the method of radius of gyration is impossible for a single Cluster–Cluster Aggregates composed of small number of the constituent particles, and partly because we assume the two point correlation function given by Eq. (8). Thus the derived fractal dimensions $D_{\rm f}$ may not necessarily represent the real fractal dimension of the dust aggregates, but are reasonable values with an exception for the smallest BCCA aggregate with $N = 256$. The value of the cutoff parameter ξ simply reflects the size of the scattering body. It might be noted that the derived values of ξR are roughly consistent with the geometric cross section equivalent radii tabulated in Table 1.

The scattered intensity of BPCA by DDA calculations cannot be reproduced by the model B with a set of the fitting parameters $D_{\rm f}$ and ξ. With the fitting parameters tabulated in Table 1 we can reproduce the scattered intensity in the region well fit-

ted by the model A, but the calculated scattered intensity is too large in the backward directions for the large sized BPCA (see Fig. 4b). The derived fractal dimensions $D_{\rm f}$ are 3 in agreement with the fractal dimension D calculated by the method of radius of gyration in the limit of large size, irrespective of the number of constituent particles. The values of the cutoff parameter are ~ 0.38 , but the deduced size of the scattering body does not correspond to the sizes that characterize the aggregates. When sacrificing the fitting in the region of $q \lesssim 2$ (the diffraction lobe of the large sized aggregates), the model B reproduces the scattered intensity of BPCA in the backward directions (in the region of $q \gtrsim 5$) with the fitting parameters $D_{\rm f} \sim 2.5$ and $\xi \sim 1$ corresponding to the characteristic radius of aggregates. If the scattered intensity in the backward directions would be dominated by the single scattered light from the surface region of the large sized aggregates, this might suggest the heterogeneous structure of BPCA derived from the analysis of the inner structure of the aggregates (Blum and Kozasa, unpublished data); the uniform inner core and the surface region with outwardly decreasing density.

The model B neglecting the effect of multiple scattering can reproduce angular dependence of the scattered intensity of BCCA with a set of reasonable fitting parameters $D_{\rm f}$ and ξ, but cannot for BPCA. BPCA are characterized by denser and more homogeneous structure in comparison with BCCA. As discussed in Sect. 3, the multiple scattering is more dominant in BPCA than in BCCA as the size of the aggregates increases. Therefore the effect of multiple scattering is considered to be the reason why we cannot reproduce the behavior of the scattered intensity of BPCA by the model B with a set of the fitting parameters. So the randomly scattered light due to the multiple scattering in BPCA more destructively interferes each other in comparison with BCCA. Resultingly, following the region of coherent scattering the scattered intensity is diminished sharply, and this causes the remarkable forward scattering lobe to develop in spite of the smaller size than BCCA with the same number of constituent particles. The effect of multiple scattering can be confirmed by the fact that the scattered intensity in the region of $2.4 \lesssim q \lesssim 5$ is significantly depressed in magnetite BPCA than in silicate ones as the number of constituent particles N increases.

The result of DDA calculation and comparison with the simple models being referred, we can divide the angular dependence of the scattered intensity into at least 4 regimes according to the nondimensional value q when the size parameter of aggregate $X \gtrsim 3$. The behavior of the angular dependence of the scattered intensity can be summarized qualitatively as follows: (1) In the region of $q = 2kR\sin(\theta/2) \lesssim 2$, the scattered light is dominated by the coherently scattered light from the individual constituent particles, and form the "diffraction lobe". The shape and intensity of the "diffraction lobe" well reflect the size as well as the mass of the dust aggregates. (2) With increasing q, the incoherently scattered light becomes dominant and the scattered intensity decreases in proportion to $q^{-\gamma}$. In the region of $2.4 \lesssim q \lesssim 5.0$ the behavior of scattered intensity reflects the structure of dust aggregates through the effect of multiple scattering in aggregates. In a dense media such as BPCA, the incoherently scattered light efficiently interferes each other, which causes the forward scattering lobe to develop. The value γ ranges from ~ 5 to ~ 6 for BPCA reflecting the dense structure, and from ~ 1.5 to ~ 2 for BCCA reflecting the very porous structure. (3) In the region of $5.0 \lesssim q \lesssim q_c$, the scattered intensity is proportional to q^{-3}, irrespective of the structure of the aggregates. The intensity oscillates as the size of the aggregates increases. The dividing value q_c increases with increasing size of dust aggregates. (4) In the backward directions of $q \gtrsim q_c$, the scattering is almost isotropic with oscillations and a significant enhancement of backward scattering as the size of aggregates increases.

In the region of $q \gtrsim 5$, the angular dependence of the scattered intensity exhibits the similar behavior regardless of the structure of aggregates. This seems to suggest that the scattering process in this region is dominated by the single scattering. However the scattered intensity in this region is more depressed in BPCA than in BCCA with the same number of constituent particles. We cannot clarify from the results of present calculations what reflects to the behavior of the scattered intensity in this region.

The classification of the behavior of scattered intensity according to the value q described above is true for dust aggregates consisting of the constituent particles whose radii satisfy the condition for the application of the discrete dipole method. It should be investigated theoretically as well as experimentally how the angular dependence of the scattered intensity reflects the size and structure of dust aggregates composed of constituent particles whose size parameters $x = ka_0 \gtrsim 1$. Anyway the result of our calculations suggests that the angular dependence of the scattered intensity is a useful indicator of the size and the structure of the aggregates almost irrespective of the chemical composition when the scattered intensity is measured by covering a wide range of scattering angles.

5. Concluding remarks

The angular dependence of the scattered light has been investigated systematically by using the discrete dipole method in order to reveal the dependence of the behavior of the scattered light on the structure, size and chemical composition of dust aggregates. The angular dependence of the scattered light shows the same duality as that observed from the zodiacal light and as that measured in the laboratories when Mie theory is applied to interpret the result. The the details of the angular dependence is sensitive to the difference in the structure as well as in the chemical composition of dust aggregates as the number of constituent particle increases.

The behavior of linear polarization depends not only on the chemical composition but also on the structure and size of aggregates. The behavior seems to be related with the effect of multiple scattering in aggregates reflecting their structure and size. However it is not so simple to interpret the behavior quantitatively in relation to the characteristics of the aggregates.

The angular dependence of the scattered intensity well reflects the size and structure of the dust aggregates almost irrespective of the chemical composition. The behavior of the angular dependence of the scattered light can be divided into at least 4 regimes according to the value of the dimensionless quantity $q = 2kR\sin(\theta/2)$ when the size parameter of aggregate $X \gtrsim 3$: In the region of $q \lesssim 2$, the angular dependence is not sensitive to the structure of the aggregates. The shape and intensity of the "diffraction lobe" arising from the coherent scattering from scatterers well reflect the size as well as the mass of dust aggregates irrespective of the structure and the chemical composition. As the value of q increases, the scattered intensity decreases in proportion to $q^{-\gamma}$. In the region followed by the "diffraction lobe" the value of γ depends on the structure of dust aggregates through the effect of multiple scattering. After then, irrespective of the structure of the aggregates the scattered intensity decreases in proportion to q^{-3} with oscillations as the size of aggregates increases. In backward directions the scattering tends to be isotropic accompanied with oscillations and a significant enhancement of backward scattering with increasing size of aggregates. The dividing value of q between the region of power law dependence and the region of isotropic scattering increases as the size of aggregates increases.

The dust aggregates treated in this paper cannot reproduce the behavior of observed linear polarization; the maximum value of the linear polarization ~ 0.3 at around $\theta = 90°$ for the zodiacal light (see Giese et al. 1978 for the references) and the negative polarization in the backward directions for the scattered light from cometary atmospheres (see Dollfus 1989 for the references). It is still unclear what kinds of dust aggregates produce such characteristic features. The results of our calculations show that the scattering properties, in particular the degree of linear polarization, not only depends on the chemical composition but also strongly depends on the structure as well as the size of the dust aggregates. More extended experimental and theoretical investigations are needed with control on the parameters that characterize the dust aggregates in order to relate the scattering properties to the structure, size and chemical composition quantitatively.

Acknowledgements. We thank Dr. A. N. Witt, the referee, for helpful comments on improving the manuscript, and thank Dr. B. T. Draine for providing us the original program of the discrete dipole approximation. T. K. is grateful to Profs. H. Fechtig and H. J. Völk for their hospitality during his stay at the Max–Planck–Institut für Kernphysik, and is also grateful to Dr. T. Yamamoto for his kindness at ISAS. J. B. is supported by the Deutsche Forschungsgemeinshaft under grant Ig 3/13–4. T. M. acknowledges the support from the Scientific Research Fund of the Ministry of Education, Science, and Culture (04835011). The numerical calculations were performed partly by using Vax–Stations 3100, 3600 and 8650 at MPI–K, and partly by using FACOM VP–200 at ISAS and FACOM M–780 at NAOMTK.

References

Berry, M. V., Percival, I. C., 1986, Optica Acta 33, 577
Bohren, C. F., Huffman, D. R., 1983, Absorption and Scattering of Light by Small Particles, John Wiley & Sons, New York
Brownlee, D. E., Tomandl, D. A., Hodge, P. W., 1976, in: Elsässer, H., Fechtig, H (eds.) IAU. Colloq. 31, Interplanetary Dust and Zodiacal Light, Springer–Verlag, Berlin, p. 279
Cardelli, J. A., Clayton, G. C., Mathis, J. S., 1989, ApJ 345, 245
Dollfus, A., 1989, A&A 213, 469
Draine, B. T., 1988, ApJ 333, 848
Draine, B. T., 1990, in: Blitz, L. (ed.) The Evolution of Interstellar Medium, Astron. Soc. of the Pacific Conference Series, San Francisco, Vol. 12, p. 245
Draine, B. T., Goodman, J. J. 1993, ApJ 405, 685
Giese, R. H., Weiss, K., Zerull, R. H., Ono, T., 1978, A&A 65, 265
Greenberg, J. M., Hage, J. I., 1990, ApJ 361, 260
Goodman, J. J., Draine, B. T., Flatau, P. J., 1991, Optics Letters 16, 1198
Hage, J. I., 1990, Ph. D. thesis, Univ. of Leiden, the Netherlands
Hage, J. I., Greenberg, J. M., 1990, ApJ 361, 251
Hage, J. I., Greenberg, J. M., Wang, R. T., 1991, Appl. Optics 30, 1141
Kozasa, T., Blum, J., Mukai, T., 1992, A&A 263, 423 (Paper I)
Mathis, J. S., 1990, ARA&A 28, 37
Mukai, T., 1990, in: Bonetti, A., Greenberg, J. M., Aliello, S. (eds.) Evolution of Interstellar Dust and Related Topics, Elsevier, Publishers B. V., North–Holland, p. 397
Mukai, T., Ishimoto, H., Kozasa, T., Blum, J., Greenberg, J. M., 1992, A&A 262, 315
Perrin, J. M., Sivan, J. P., 1991, A&A 247, 497
Teixeira, J., 1986, in: Stanley, E. H., Ostrowsky, N. (eds.) On Growth and Form, NATO ASI Series No. 100, Martinus Nijhoff Publishers, Dordrecht, p. 145
Weiss–Wrana, K., 1983, A&A 126, 240
West, R. A., 1991a, Icarus 90, 330
West, R. A., 1991b, Appl. Optics 30, 5316
Zerull, R. H., Gustafson, B. Å. S., Schulz, K., Thiele–Corbach, E., 1992, preprint

This article was processed by the author using Springer-Verlag TEX A&A macro package 1992.